

β -Decamethoxysapphyrin and Its *N*-Benzyl Analogue

Anup Rana,^{†,‡} B. Sathish Kumar,[†] and Pradeepta K. Panda^{*,†,‡}

[†]School of Chemistry and [‡]Advanced Centre of Research in High Energy Materials, University of Hyderabad, Hyderabad 500046, India

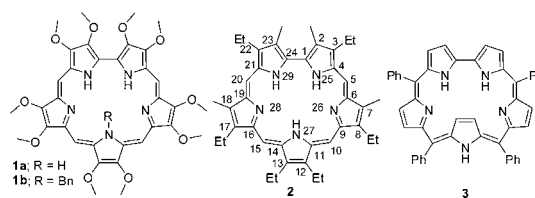
S Supporting Information

ABSTRACT: The synthesis of a highly electron-rich decamethoxysapphyrin and its 27-*N*-benzyl analogue is reported for the first time. The effects of β -methoxy and 27-*N*-benzyl substitution on structure, anion binding, absorption, and electrochemical properties were explored in detail. Upon 27-*N*-benzyl substitution, counteranion-induced structural deformation arises in the diprotonated state, which could be clearly noticed both in solution ¹H NMR study and solid-state structural analysis. This type of anion-induced structural deformation is noted for the first time in β -substituted sapphyrins. Further, the free base sapphyrins generate singlet oxygen with moderate efficiency (~42%); hence, they may act as good photosensitizers.



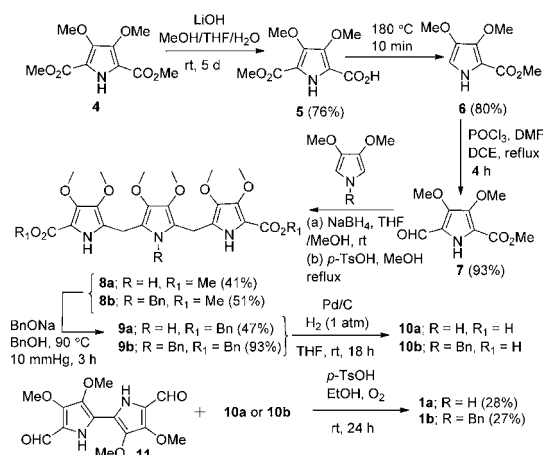
Sapphyrin is the first reported expanded porphyrin, and it has gained much attention as a versatile anion binding agent.¹ In addition, it has also been explored as a photodynamic therapeutic agent and recently as a third-order nonlinear optical material.² Further, this system can exhibit structural diversity due to inversion of the pyrrole unit opposite the bipyrrrole moiety, a property that was first observed by Latos-Grażyński for tetraphenylsapphyrin 3.³ Though initial research was confined to decaalkylated and *meso*-arylated sapphyrins, many modified sapphyrins were later synthesized, including all aza cores of sapphyrin modified with other heteroatom (C, O, S, and Se), *N*-confused, *N*-fused, and π -expanded sapphyrins.⁴ However, functionalization of sapphyrin at its β -positions is very limited, particularly owing to the difficulties associated with the synthesis of the building blocks. In this regard, Sessler and co-workers reported 2,3,22,23-tetramethoxy-substituted sapphyrin following the “3 + 1 + 1” approach.⁵ Recently, we have reported β -octamethoxyporphycene,⁶ which shows good hydrophilicity and efficient singlet oxygen quantum yield upon metalation, and this motivated us to take up the challenge to synthesize the decamethoxy analogue of sapphyrin. As this sapphyrin is expected to be highly basic in nature owing to the presence of ten electron-donating methoxy groups at its periphery, we therefore expected it to show interesting host–guest attributes both as a free base and also in its diprotonated state. Herein, we report the synthesis of β -decamethoxysapphyrin 1a and its anion-binding studies. In addition, the 27-*N*-benzyl analogue 1b was also synthesized in order to explore the possible structural consequences resulting from probable disposition of the benzyl group in the free base and, more importantly, its interaction with the incoming anions in its diprotonated state.

The synthesis of sapphyrins was achieved by following conventional “3 + 2” McDonald-type acid-catalyzed condensation of bipyrrrole dialdehyde and tripyrrane diacid. Recently, we have reported the synthesis of tetramethoxybipyrrrole dicarbaldehyde 11;⁶ therefore, in order to achieve our target, our focus was on the synthesis of precursor hexamethoxytripyrane



dicarboxylic acid 10 (Scheme 1). The synthesis of 10 started with hydrolysis of one methyl ester group of dimethyl 3,4-

Scheme 1. Synthesis of β -Decamethoxysapphyrins



dimethoxypyrrole-2,5-dicarboxylate 4⁷ with LiOH (1 equiv) to obtain the mono-de-esterified product 5 in 76% yield,⁸ followed by heating of 5 at 180 °C under nitrogen atmosphere, which led to the formation of α -free pyrrole derivative 6 in 80% yield. Subsequent Vilsmeier–Haack formylation of 6 provided the

Received: May 4, 2015

Published: June 5, 2015

desired aldehyde derivative **7** in 93% yield. Further, reduction of **7** with sodium borohydride provided methyl 5-(hydroxymethyl)-3,4-dimethoxypyrrrole-2-carboxylate, which was used immediately for acid-catalyzed condensation with 3,4-dimethoxypyrrrole or its *N*-benzyl analogue under reflux conditions, in MeOH to provide the desired tripyrrane diesters **8a** and **8b** in 41 and 51% yields, respectively.⁹ Further, transesterification of diesters **8a** and **8b** was performed in the presence of sodium benzyloxide in benzyl alcohol to obtain corresponding dibenzyl esters **9a** and **9b** in 47 and 93% yields, respectively.¹⁰ It is noteworthy to mention that the traditional method to synthesize tripyrrane dibenzyl ester using benzyl pyrrole-2-carboxylate (employing transesterification of **6** before condensation) led to comparatively poor overall yield along with a tedious purification process in the case of **9a**. Hydrogenolysis of benzyl esters (**9a** and **9b**) was carried out with Pd/C/H₂ in THF, leading to the corresponding tripyrrane diacids **10a** and **10b**, which were used immediately for the next step. With both starting materials in hand, “3 + 2”-type McDonald condensation of tetramethoxybipyrrole dialdehyde **11** and hexamethoxytripyrane diacid (**10a** or **10b**) in the presence of *p*-TsOH.H₂O in EtOH with continuous bubbling of oxygen provided the desired decamethoxysapphyrins **1a** and **1b** in 28 and 27% yields, respectively. The diprotonated salts were prepared by washing a dichloromethane solution of free-base sapphyrins **1a** and **1b** with the corresponding acids. All of the precursors and final products were characterized by standard spectroscopic techniques.

The ¹H NMR spectrum of **1a** consists of *meso* protons at 10.98, 10.71 ppm and an NH signal at −5.88 ppm, which is more deshielded and shielded, respectively, compared to sapphyrin **2**.¹¹ Further, the position of NH signal varies with the amount of water present in CDCl₃. The large shielding of NH signals in **1a** compared to **2**, along with concomitant absence of any weak NH signals, indicates fast water-assisted NH tautomerization on the NMR time scale.^{2c,11} The protonation of free base sapphyrin **1a** led to formation of diprotonated salt, where the *meso* protons were downfield shifted (~1 ppm) and three sets of NH signals appeared with 1:2:2 ratios ranging from −5.42 to −7.67 ppm. Minimal change was observed in the *meso*-proton signals of various diprotonated salts, but NH resonances vary widely, depending on counteranions, probably arising from varied interactions of counteranions with diprotonated sapphyrin (Table S1, Supporting Information (SI)). A similar trend was observed in the ¹H NMR spectrum of *N*-benzylsapphyrin **1b**, consisting of *meso* protons at 10.97, 10.96 and NH at −2.43 ppm, which clearly indicates that *N*-benzyl substitution at the 27-position did not affect the aromaticity, symmetry, and planarity of the macrocycle. Most importantly, the benzyl group was situated inside the core of the macrocycle, confirmed by a large upfield shift of the benzyl −CH₂ proton signal (−6.6 ppm) along with phenyl protons. The *meso* protons were downfield shifted (~1 ppm), and NH protons appeared in the range of −4.60 to −6.91 ppm depending on the counteranions, with a 2:2 ratio for diprotonated salts of **1b** (SI, Table S1). Again, the benzylic CH₂ protons reside in the upfield region, indicating that the diprotonated salts also display all-*N* in the conformer, in spite of the presence of the bulky 27-*N*-benzyl substituent. However, the position of protons from the benzyl moiety varies with counteranions, probably arising from the steric or/and electronic repulsion (anion- π interaction) of it with an incoming counteranion toward the macrocyclic core. Among the studied diprotonated salts, a maximum downfield shift was observed for *o*-CH, followed by *m*-CH > −CH₂ (determined by D₂O

exchange) > *p*-CH in the benzyl group (Figure S32 and Table S1, SI). If we compare displacement of *N*-benzylpyrrole signals of dipicrate **1b**·2PA, dichloride **1b**·2HCl, and dibromide **1b**·2HBr salts by ¹H NMR, the order is **1b**·2PA < **1b**·2HBr < **1b**·2HCl, which clearly indicates the bulky counteranions remain away from macrocyclic core leading to minimal distortion of the structure. The ditrifluoroacetate **1b**·2TFA salt shows a higher degree of displacement compared to **1b**·2PA due to its less bulky nature. The maximum displacement of the *N*-benzylpyrrole moiety is observed for the diperchlorate **1b**·2HClO₄ salt, which is preceded the di-*p*-toluenesulfonate **1b**·2PTSA salt, probably owing to the relatively more bulky nature of the TsO[−] ion. Notably, we have observed that there is an equilibrium between the planar and nonplanar macrocyclic core, which is more evident in the case of **1b**·2HClO₄ and **1b**·2PA (small peaks were observed, where *meso* protons were more downfield shifted and benzylic CH₂ more upfield shifted compared to the major contributing part) (Figures S28 and S29, SI). Therefore, from the above results, we can conclude that the counteranion-induced displacement of the *N*-benzylpyrrole moiety opposite to the bipyrrole unit depends on the size of the counteranions. However, the complete inversion of *N*-benzylpyrrole moiety did not occur, probably due to the presence of β -methoxy substituents.

The UV–vis absorption of free-base sapphyrin **1a** consists of Soret band at 449 nm and four Q-type bands at 586, 632, 647, and 720 nm (Figure 1). Further, protonation of **1a** with HClO₄

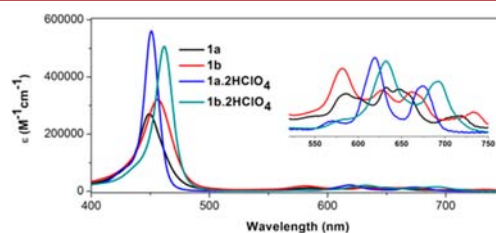


Figure 1. UV–vis spectra of **1a**, **1b**, and their perchlorate salts in CHCl₃ at 25 °C. Inset represents enlarged Q-bands.

leads to large intensification of Soret band and Q-bands. Minimal shift in the Soret band was observed (only 2 nm red shift); however, the increased symmetry led to two characteristic blue-shifted Q-bands at 619 and 674 nm compared to free base **1a**. The free-base sapphyrin **1a** and its diprotonated salts display emission with maxima at 724 and 679–688 nm, respectively (Figure S34, SI). Enhancement of the fluorescence quantum yield for diprotonated salts (ϕ_f , 0.029–0.067) compared to free base **1a** (ϕ_f , 0.017) may be attributed to the reduced intramolecular charge transfer upon protonation¹² and the more rigid structure of the former along with the absence of tautomerism (Table S2, SI). Similarly, the UV–vis spectrum of free base **1b** consists of a Soret band at 456 nm and four Q-bands at 582, 626, 662, and 732 nm (in CHCl₃), where Soret and the lowest energy Q-bands are 7 and 12 nm red-shifted, respectively, compared to **1a** due to the distortion of the core induced by the *N*-benzyl substituent (Figure 1). More interestingly, Q-bands of **1b** show a four-banded pattern, more generally noticed in free base porphyrins, which, however, is quite unexpected in sapphyrin chemistry. This may be attributed to the lesser number of tautomers (four only) upon *N*-benzylation at the 27-position (in **1b**) compared to free-base sapphyrins (six). Protonation of **1b** leads to a red-shifted Soret band (2–6 nm)

and blue-shifted two Q-type bands in the range of 626–693 nm (Figures 1 and S33, SI). Again, free base **1b** and its diprotonated salts weakly emit with emission maxima at 739 and ~697 nm, respectively (Figure S34, SI). The reduced fluorescence quantum yield of diprotonated salts (0.005–0.017) compared to free base **1b** probably arises due to the distortion of core of the macrocycle caused by steric interaction between the counteranion and benzyl moiety, as evidenced by the ^1H NMR studies (Table S2, SI). Both free bases **1a** and **1b** generate singlet oxygen in aerated toluene with moderate efficiencies (ϕ_{Δ} , 0.44 for **1a** and 0.42 for **1b**), making them useful as possible photosensitizers for deep-site PDT (Figures S35 and S36, SI).

The protonation of free base sapphyrins **1a** and **1b** studied by successive addition of TFA in dichloromethane solution leads to an increase in the intensity of the Soret band with minimal red shift, whereas the four Q-bands reduce to two blue-shifted bands (Figures S37 and S38, SI). Also, in both cases, the intensity of the Soret band undergoes saturation after addition of ~6 equiv of TFA, and no further change was observed even after addition of excess TFA. In addition, owing to the strong basicity of these sapphyrins, we could observe diprotonation even with a weak acid like acetic acid, albeit upon addition of much higher equivalents (Figures S39 and S40, SI).

The anion-binding study of diprotonated salts **1a**·2HF, **1a**·2HCl, and **1a**·2HBr was carried out in methanol by a UV–vis spectroscopic method (Figures S41–S44, SI). The absorption spectra display a Soret band at 443 nm and two Q-bands at 614 and 661 nm in all cases, revealing that sapphyrin **1a** exists in planar diprotonated form, whereas anions are solvated in methanol (Figure S33, SI). The binding studies were carried out with tetrabutylammonium (TBA) salts of fluoride, chloride, and bromide ions. Successive addition of TBAF to **1a**·2HF leads to a decrease in intensity of the Soret band, with a new peak evolving around ~416 nm (Figure S41, SI). The binding constant was measured by the Connor equation, which could nicely fit with 1:1 binding stoichiometry, which was further confirmed by Job's plot analysis (Figure S42, SI). Owing to the increased basicity, protonated sapphyrin **1a** binds selectively with fluoride ion only, although with reduced affinity (K_a $1.03 \times 10^5 \text{ M}^{-1}$), compared to decaalkylated sapphyrin **2**·2HF (K_a $2.8 \times 10^5 \text{ M}^{-1}$).¹³ On the other hand, the much anticipated anion-binding behavior for diprotonated **1b** owing to the presence of the 27-*N*-benzyl substituent could not be realized, as we could not achieve the diprotonated **1b**·2HF salt using 10% HF (only monoprotonated salt formed) and the deprotonation of **1b**·2HCl and **1b**·2HBr salts in methanol.

The structure of sapphyrin **1a**·2PTSA was further characterized by single-crystal XRD techniques (Figure 2) and exhibits a near-planar macrocyclic core where two *p*-TsO[−] ions resided symmetrically (distance of O of *p*-TsO[−] from mean plane, 1.35 Å). Further, each *p*-TsO[−] unit is hydrogen bonded to three pyrrolic moieties with N···O distances ranging from 2.83 to 3.07 Å. The distance between N2–N4 units is 5.43 Å, which is quite similar to that of **2**·2HCl (5.50 Å).¹³ Similarly, the structures of sapphyrins **1b**·2HClO₄ and **1b**·PTSA were also characterized. The asymmetric unit of **1b**·2HClO₄ consists of three diprotonated sapphyrin units (Figure S46, SI). The presence of an *N*-benzyl substituent at the 27-position leads to distortion of the macrocyclic core (Figure 2). More strikingly, structural parameters of all three sapphyrin units are found to be different from each other, with the N2–N4 distance in the range from 5.31 to 5.41 Å. Owing to its unique structure, two perchlorate units are asymmetrically disposed in **1b**·2HClO₄, where the compara-

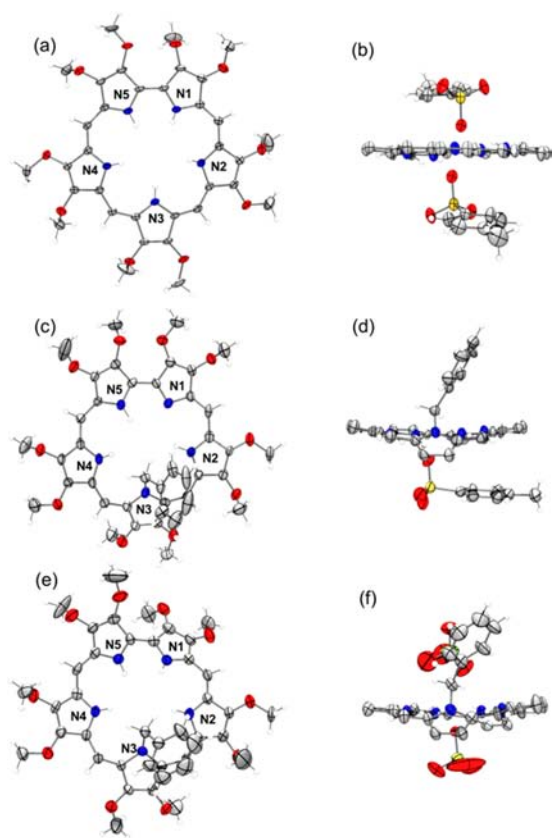


Figure 2. Molecular structures of (a) front and (b) side view of **1a**·2PTSA, (c) front and (d) side view of **1b**·PTSA, and (e) front and (f) side view of **1b**·2HClO₄, scaled at 35% probability level. In the front view counteranions and in side view methoxy groups are removed for clarity. Color code: C, gray; N, blue; O, red; S, yellow; Cl, yellow green; H, white.

tively nearer ClO₄[−] unit (distance from mean plane 0.92 Å) hydrogen bonded with four pyrrole NHs and the unit farther away (distance from mean plane 2.48 Å) H-bonded with only one pyrrole NH (Figure S45, SI). Interestingly, the nearer ClO₄[−] unit resided in the center of the core with an N···O distance ~2.93 Å, revealing a stronger H-bonded interaction. Also, further ruffling of the structure occurs due to a nonbonding interaction between the ClO₄[−] ion with the benzyl unit. The maximum displacement of β -C's of the N3-pyrrole unit from the mean plane drawn through the N1, N2, N4, and N5 units is 1.29 Å, and the maximum angle between mean planes drawn through the N1, N2, N4 and N5, and N3-pyrrole units excluding the benzyl group is 36.22°. The above result proves our previous assumption of ^1H NMR studies that approach of the ClO₄[−] ion toward the macrocyclic core leads to flipping of the benzyl-substituted N3-pyrrole unit. On the other hand, the N2–N4 distance (5.46 Å) for sapphyrin **1b**·PTSA is similar to that of **1a**·2PTSA and slightly wider compared to that in the case of **1b**·2HClO₄ (Figure 2). Further, the *p*-TsO[−] unit hydrogen bonded with N4 and N5 pyrrolic units with an O···N distance ~2.77 Å and the distance from the mean plane drawn through the macrocycle excluding the benzyl and methoxy group is 1.40 Å. Similar to **1b**·2HClO₄, the flipping of the *N*-benzylpyrrole unit from the macrocyclic plane is clearly evident from the maximum displacement of β -C's of the N3-pyrrole unit from the mean plane drawn through N1, N2, N4, and N5 is 1.18 Å, which is 0.11 Å lower compared to **1b**·2HClO₄. Further, the angle between mean plane drawn through

N1, N2, N4, and N5 and the N3-pyrrole unit is 31.87°. Therefore, from the above structural data we can conclude that one of the counterions plays a major role in the out-of-plane displacement of the *N*-benzylpyrrole unit, and this could be correlated with ¹H NMR analysis.

Electrochemical measurements of free-base sapphyrins **1a** and **1b** and their perchlorate salts were carried out by cyclic voltammetry (CV) and differential pulse voltammetry (DPV) in DCM (Figures S47–51, SI, and Table 1). Notably, there are

Table 1. Comparative Oxidation and Reduction Potentials (V vs Ag/AgCl) for Sapphyrins and Their Perchlorate Salts

sapphyrins	reduction	oxidation
1a	−1.16 ^a	+0.56, ^a +1.04, +1.23
1b	−1.30 ^a	+0.48, ^a +0.86, ^a +1.22
1a ·2HClO ₄	−1.09, −0.86, −0.74 ^a	+1.23
1b ·2HClO ₄	−1.20, −0.76, −0.61	+1.24

^aMeasured by DPV.

very few reports on the electrochemical properties of sapphyrins^{13,14} until recently, when Kadish and co-workers reported a detailed electrochemical study of *meso*-tetraarylsapphyrins.¹⁵ We observed three reversible and/or quasi-reversible oxidation potentials and one detectable irreversible reduction potential for free-base sapphyrins **1a** and **1b**. We could notice only one reduction potential at −1.16 and −1.30 V for **1a** and **1b**, respectively, whereas the oxidation potentials of free-base sapphyrins may be attributed to the formation of π -cation radical, dicationic species, and tricationic species. The first oxidations were observed at +0.56 and +0.48 V, respectively, for **1a** and **1b**. On the other hand, diprotonated sapphyrins, i.e., **1a**·2HClO₄ and **1b**·2HClO₄, display one oxidation and three reduction potentials (all reversible). Most interestingly, protonation leads to the disappearance of first two oxidation potentials of free base sapphyrins and then the appearance of two more reversible reduction potentials. In addition, the third oxidation potential of free base and the oxidation potential of the diprotonated salts are very similar, indicating that probably they originated from the same electrochemical oxidation states. The chemically generated diprotonated state of sapphyrins leads to the disappearance of first two oxidation potentials and then the appearance of two more reductions at more positive potentials, which may arise from electrochemically induced successive deprotonations of diprotonated sapphyrins. A similar type of trend was also observed by Kadish and co-workers for tetraarylsapphyrins.^{15b} Further, the third reduction potential of diprotonated sapphyrins probably evolved from the generation of sapphyrin anion radical species. However, further detailed studies are needed to understand these interesting electrochemical properties of sapphyrins and their diprotonated salts.

In conclusion, we have synthesized and characterized β -decamethoxysapphyrin and its 27-*N*-benzyl analogue along with their various diprotonated salts. Among them, diprotonated **1a** binds selectively with fluoride ion in methanol. Both **1a** and **1b** generate singlet oxygen with moderate yield and, hence, may find application as good photosensitizers. Electrochemical studies of **1a** and **1b** and their perchlorate salts provide important information about electronic properties of both free-base and protonated sapphyrins. Most interestingly, both ¹H NMR studies and solid-state characterization of diprotonated **1b** reveal anion-induced out-of-plane deformation of the *N*-benzylpyrrole unit for the first time. This unravels a new way to control the anion-

binding event in sapphyrins and with appropriate substituents may lead to exciting results. Our present efforts are being directed toward this goal.

■ ASSOCIATED CONTENT

Supporting Information

Detailed synthetic procedure, NMR, photophysical, crystallographic, electrochemical data, and crystal data (CIF) (CCDC 1047320–1047322). The Supporting Information is available free of charge on the ACS Publications website at DOI: 10.1021/acs.orglett.5b01306.

■ AUTHOR INFORMATION

Corresponding Author

*E-mail: pkpsc@uohyd.ernet.in, pradeepta.panda@gmail.com.

Notes

The authors declare no competing financial interest.

■ ACKNOWLEDGMENTS

This work was supported by UGC, India (Project no. 41-263/2012 (SR)). A.R. and B.S.K. thank CSIR, India, for fellowships, and A.R. also thanks DRDO, India, for financial assistance. We thank Dr. Ranjit Thakuria, Assistant Professor, Department of Chemistry, University of Gauhati, India, for refining the crystal structures.

■ REFERENCES

- Sessler, J. L.; Davis, J. M. *Acc. Chem. Res.* **2001**, *34*, 989.
- (a) Maiya, B. G.; Cyr, M.; Harriman, A.; Sessler, J. L. *J. Phys. Chem.* **1990**, *94*, 3597. (b) Hooker, J. D.; Nguyen, V. H.; Taylor, V. M.; Cedeño, D. L.; Lash, T. D.; Jones, M. A.; Robledo, S. M.; Vélez, I. D. *Photochem. Photobiol.* **2012**, *88*, 194. (c) Sarma, T.; Anusha, P. T.; Pabbathi, A.; Rao, S. V.; Panda, P. K. *Chem.—Eur. J.* **2014**, *20*, 15561.
- Chmielewski, P. J.; Latos-Grażyński, L.; Rachlewicz, K. *Chem.—Eur. J.* **1995**, *1*, 68.
- (a) Misra, R.; Chandrashekar, T. K. *Acc. Chem. Res.* **2008**, *41*, 265. (b) Sessler, J. L.; Cho, D.-G.; Stępień, M.; Lynch, V.; Waluk, J.; Yoon, Z. S.; Kim, D. *J. Am. Chem. Soc.* **2006**, *128*, 12640. (c) Lash, T. D.; Richter, D. T. *J. Am. Chem. Soc.* **1998**, *120*, 9965. (d) Gupta, I.; Srinivasan, A.; Morimoto, T.; Toganoh, M.; Furuta, H. *Angew. Chem., Int. Ed.* **2008**, *47*, 4563. (e) Okujima, T.; Kikkawa, T.; Kawakami, S.; Shimizu, Y.; Yamada, H.; Ono, N.; Uno, H. *Tetrahedron* **2010**, *66*, 7213. (f) Panda, P. K.; Kang, Y.-J.; Lee, C.-H. *Angew. Chem., Int. Ed.* **2005**, *44*, 4053. (g) Cho, D.-G.; Plitt, P.; Kim, S. K.; Lynch, V.; Hong, S.-J.; Lee, C.-H.; Sessler, J. L. *J. Am. Chem. Soc.* **2008**, *130*, 10502.
- Shevchuk, S. V.; Davis, J. M.; Sessler, J. L. *Tetrahedron Lett.* **2001**, *42*, 2447.
- Rana, A.; Panda, P. K. *Org. Lett.* **2014**, *16*, 78.
- Merz, A.; Schropp, R.; Dötterl, E. *Synthesis* **1995**, 795.
- Boger, D. L.; Patel, M. *J. Org. Chem.* **1988**, *53*, 1405.
- Uno, H.; Nakamoto, K.-i.; Kuroki, K.; Fujimoto, A.; Ono, N. *Chem.—Eur. J.* **2007**, *13*, 5773.
- Boudif, A.; Momenteau, M. *J. Chem. Soc., Perkin Trans. 1* **1996**, 1235.
- Rachlewicz, K.; Latos-Grażyński, L.; Gebauer, A.; Vivian, A.; Sessler, J. L. *J. Chem. Soc., Perkin Trans. 2* **1999**, 2189.
- Rana, A.; Lee, S.; Kim, D.; Panda, P. K. *Chem. Commun.* **2015**, *51*, 7705.
- Shionoya, M.; Furuta, H.; Lynch, V.; Harriman, A.; Sessler, J. L. *J. Am. Chem. Soc.* **1992**, *114*, 5714.
- Kang, S.; Hayashi, H.; Umeyama, T.; Matano, Y.; Tkachenko, N. V.; Lemmetynen, H.; Imahori, H. *Chem.—Asian J.* **2008**, *3*, 2065.
- (a) Yuan, M.; Ou, Z.; Fang, Y.; Huang, S.; Xue, Z.; Lu, G.; Kadish, K. M. *Inorg. Chem.* **2013**, *52*, 6664. (b) Ou, Z.; Meng, D.; Yuan, M.; Huang, W.; Fang, Y.; Kadish, K. M. *J. Phys. Chem. B* **2013**, *117*, 13646.